THE NATIONAL RADIO ASTRONOMY OBSERVATORY

SOCORRO, NEW MEXICO

VERY LARGE ARRAY PROGRAM

VLA ELECTRONICS MEMORANDUM NO. 196

AN ANALYSIS OF THE VLA F/R DRIVE DYNAMICS

D. Weber and S. Christiansen

September 1980

Suggested background music: "Four Seasons" by Vivaldi.

1.0 INTRODUCTION

This memorandum describes an analysis of the VLA F/R Drive that was performed to characterize the drive dynamics using actual as-built dimensions, weights, and direct measurements of motor and load torques. The analysis was undertaken to obtain a better understanding of the F/R Drive dynamics and to develop better control and fault analysis criteria for a new version of the F/R Controller that has been installed in Antenna 27. This memo also describes some of the critical controller algorithms and their application to the analysis results.

The analysis was performed by Scott Christiansen and incorporates measurements of motor drive torque and mechanism friction torque that were performed by Bill delGiudice on several antennas during the latter portion of last winter.

Cold temperature friction characteristics are of particular interest because of the frequent occurrences of drive "sticking" due to cold snaps in the winter. Friction drag measurements were requested after several antenna F/R Drives (usually focus) stuck during the observing period that followed the Christmas holidays. The sticking usually occurred after midnight, and the drive would remain stuck until mid-morning higher temperatures appeared to release the drive. Some antennas (notably #14) would stick in the daytime if they were pointed north for a period but would release a few minutes after being pointed south towards the sun.

Unfortunately, because of scheduling problems, the relatively mild weather that followed the period mentioned above, and the belated request, the measurements were made at temperatures much higher than the cold snap temperatures. The measurements were also very difficult to make because they had to be made at night on the antenna apexes. This lack of cold-temperature data has made low temperature friction drag prediction somewhat tenuous, but the calculation results roughly agree with the sticking phenomena.

Adverse weather, wind, and ice loads can also cause the F/R drive to stick; ice load sticking was observed by one of the writers (Weber) on one occasion by an inspection of the Antenna 6 F/R Mount during a sleet storm in the winter of 1977/1978. The inspection was made to determine the cause for the mechanism sticking when all the electronics and drive circuitry were functioning correctly.

The first step in the analysis involved calculation of the following classes of motor loads:

1. Physical loads and moments associated with the masses and dimensions of the moving components.
2. Loads imposed by an assumed adverse weather environment - ice, wind and rain.
3. Inertial loads and moments imposed by an assumed acceleration/velocity regime.
4. Frictional loads imposed by static, dynamic and viscous friction effects.

After calculating these loads, the total load burden was related to the torque developed by the motor to determine the torque margin and the conditions which reduce this margin to zero or stall (sticking) point.

The calculations of loads and sliding friction-inducing drag are similar to those performed in the design study by Otto Heine. (Heine did not address viscous friction).

2.0 PRINCIPAL ANALYSIS OBJECTIVES

2.1 To determine the control and fault malfuction criteria for the F/R Drive system. The results were the basis for the control and fault analysis algorithms used in the software/hardware design of the Model C F/R Controller. The base and maximum stepping rate and acceleration/deceleration characteristics of the Model B Controller were also altered as a result of the analysis.

2.2 To attempt to predict the operational envelope of the F/R Drive in terms of temperature, wind and ice loading, attitude, and deterioration of performance since the most recent major overhaul. Not all of these bounding conditions have been determined because of the difficulty of confirming measurements and the low priority of this effort.

2.3 To attempt to prevent mechanism damage by the development of fault detection schemes that can identify mechanism degradation and malfunctions. If these features had been implemented in the current controller design, the gear train damage experienced in several F/R Drives could have been avoided.

3.0 LIMITATIONS AND DEFICIENCIES OF THE ANALYSIS

3.1 Serious deficiencies exist in the detailed knowledge of the actual operating conditions in the mount; important items are: frictional drag at attitudes other than vertical and at temperatures below 40° F, effects of antenna vibration-induced errors on the position readouts, and the very erratic motion of the drives (particularly rotation) at stepping rates under ~80 Hz. Below 80 Hz a complex sequence of vibratory gear impacts propagate through the gear train and causes the drive to be very noisy (like shaking 6 rocks in a bucket) and the mechanism motion to be very jerky. This condition suggests that excessive gear and mechanism wear may result from sustained operation at low drive rates.

3.2 Very few parameters are directly available which are indicative of the state of the drive; these are: position readout, brake voltage, and brake current. By analysis of position against time and motor drive steps, it is possible to determine mechanism velocity, motor drive load, frictional drag, and sticking. Analysis of the brake voltage and current will confirm that the brake controller is operating, the values of

voltage and current are nominally correct, and the brake electrical lines are neither shorted nor open. Unfortunately, these measurements do not confirm that the brake has actually released when powered correctly.

3.3 Lost motion (slop) and vibration-induced errors on the readout were neither measured nor predicted in the calculations.

3.4 The calculations were simplistic in that we did not attempt to perform extremely accurate calculations of masses, torques, moments, and frictional loads. Pessimistic frictional coefficients were assumed (2x higher than Heine's), realizing that these coefficients are somewhat conjectural and vary with time, dust contamination and evaporation of lubricant, and the inherent cussedness of frictional phenomena.

3.5 No detailed calculations were made of viscous friction effects other than a tenuous prediction of low-temperature sticking based upon limited measurements fitted to an exponential curve. (Viscosity is a logarithmic function of temperature.) A rigorous calculation of viscous friction in these drives would require a lot of

analysis, modeling, and experimental verification. The effort required was beyond the time and manpower resources available but would have been very useful because of the dominance of viscous friction in the focus drive.

3.6 Stepper motor motion is not a smooth continuous function but is a sequence of small discrete shaft steps and velocity impulses. A rigorous analysis of the dynamics of a mechanism driven by a stepper motor would require extensive modeling and experimental verification of the models. Time and manpower resources did not permit this approach and we felt that the results of a simplistic approach would be adequate for this study. The analysis assumed that the motor drive was a smooth function, but we also determined the peak torque loads seen by the motor during step changes in drive rates.

3.7 A simple model and the associated differential equation are included in this memo to illustrate the functional behavior of the drives. We did not calculate solutions to the equation because we felt that the results would not be very useful since the mechanical design is frozen; but

it is possible to infer important dynamic relationships from the model and equations. The mechanical design is such that there are very few design changes possible; therefore the essence of the control problem is to attempt to operate the drives in a manner which maximizes system reliability, fault detection, and fault isolation.

3.8 There is no experimental data to verify that ice loaded or rusty brakes do not cause sticking. Water can penetrate the open brake mechanism and cause rusting; sleet or ice can coat the exterior and interior surfaces of the brake plate and housing. Because the brake plate travel is quite small, it appears that even a thin film of ice could inhibit release and cause cold-temperature sticking. Water penetration can cause rusting (rust stains may be seen in the vicinity of the brakes on all F/R Mounts); the brake manufacturer strongly recommends a weather protective housing for the brakes. The use of brakes which were designed for enclosed, protected environments is questionable.

3.9 The elastomer motor/drive coupling spring rate will increase with decreasing temperature which will reduce the coupling wind-up during cold

weather. This wind-up is a vital factor in the rotation drive and important in the focus drive, (see the wind-up analysis for a description of the role of wind-up in the drives). If the coupling exceeds some stiffness point the drives will not operate. We did not calculate this stiffness limit or the stiffness dependancy upon temperature.

4.0 DESCRIPTION OF THE DRIVES AND DIFFERENTIAL EQUATION OF MOTION

The F/R Mount consists of three mechanical rings, of which the top and bottom rings are fixed and the center ring is movable in two axes (see Figure 1 which depicts the F/R Mount physique). The drive motors and a portion of the drive gear train are contained in the top ring. Four shafts between the top and bottom rings function as guides for the movable ring. Drive lead screws and a splined drive shaft between the top ring and the movable ring cause the movable ring to raise or lower (focus motion) and cause the inner portion of the ring to rotate (rotation motion). Two induction brakes, mounted on the top ring, provide braking torque for the top ring gear trains to inhibit motion due to vibration or gravity forces, except during motion commands. Gears in the top ring also drive the focus and rotation readout potentiometers to indicate the position of the focus and rotation mechanism.

The focus upper-limit switch is located on the top ring; the focus lower-limit switch is located on the lower ring. The rotation-limit switches are located in a weather-proof box mounted on the movable ring.

A "barrel" is secured to the inner portion of the movable ring, and the subreflector is mounted to the base of this barrel. The barrel extends a few feet above the movable ring and has counterweights at the top to balance the barrel/subreflector around the movable ring.

The drive motors are bifilar wound, DC stepping motors with shaft rotation steps of 1.8°. The motor is coupled to the drives with an elastomer coupling that deflects as a function of the motor and drive load torques. When the system is quiescent between motion commands, the motor driver amplifiers maintain a DC current through the motor windings that develops a large motor-holding torque which locks the associated drive mechanism.

The rotation drive train has a gear ratio of 108:1 so that one motor step will produce one arc-minute of subreflector rotation. The focus drive train has a gear ratio of 2.54:1 with a lead screw pitch of .200 so that one motor step will produce 0.01 mm of sub-reflector focus motion.

Figure 1 illustrates the configuration of the F/R Mount components at the apex. Figure 2 illustrates the location of the drive motors, readout pots, and brakes

on the top ring. A simple model of the two drives is:

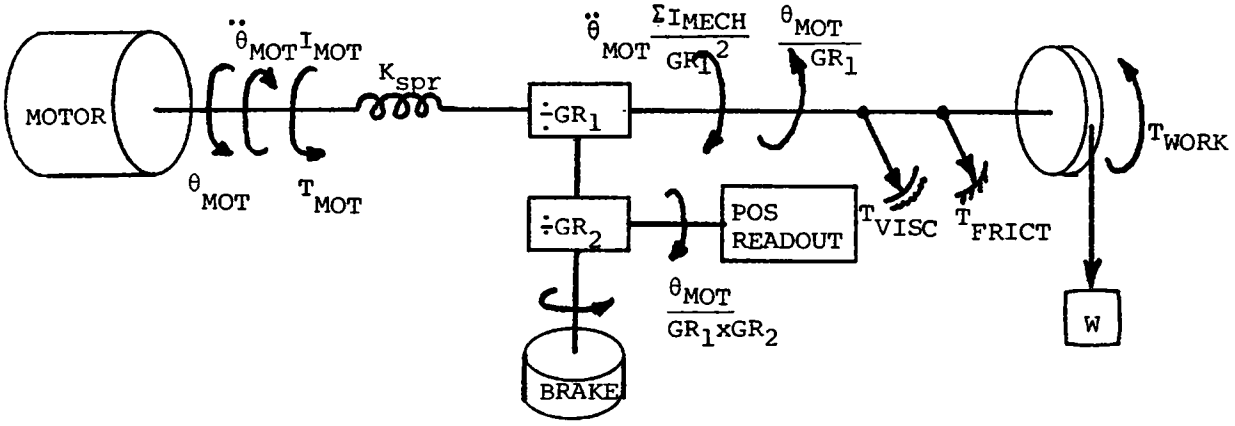

Where:

Θ_{mot} is motor shaft rotation,

T_{mot} is motor shaft torque,

I_{mot} is motor shaft moment of inertia,

K_{spr} is the spring rate of the motor drive coupling,

Σ_{mech} is the composite inertial load of the drive components at the load side of the coupling (usually referred to the motor, i.e. transformed by the gear ratio),

GR_1 is the drive gear ratio: 108:1 for rotation and 2.54:1 for focus,

$GR_1 x GR_2$ is the motor to position readout gear ratio, 15.24:1 for focus and 13.5:1 for rotation.

The differential equation of motion for this simplistic model is:

$$T_{mot} = \left(I_{mot} + \frac{K_{spr}}{GR_1^2}\,\Sigma I_{mech}\right)\ddot{\theta}_{mot} + \frac{K_{spr}}{GR_1}\,T_{visc}\,\dot{\theta}_{mot} + \frac{K_{spr}}{GR_1}\,(T_{frict} + T_{work})\,\theta_{mot}$$

The model and equation suggest an oscillatory system that is damped by viscous and coulomb friction. The step-like shaft motions can stimulate oscillatory responses when the motor stepping ratios are low enough to allow the resonance phenomena to propagate through the gear train. The resonance effects are quite complex and involve multiple impacts of gear surfaces, gear inertial loads, and coupling/gear/lead screw spring rates. The resonant frequency of the rotation drive is 8.8 Hz and 5.6 Hz for ice-free and ice-laden drives, respectively. These frequencies were calculated using a simplistic resonance equation:

$$F_{res} = \frac{1}{2\pi}\sqrt{\frac{K_{spr}}{\Sigma I_{mech}}}$$

Figure 3 graphically compares the measured drive-motor torque curve with that specified by the manufacturer, Superior Electric. The differences are striking in that the measured torque curve is square with no torque above 550 Hz, whereas the manufacturer claims a lower, flatter, and longer (i.e. higher speed range) torque curve. Both curves display a similar broad dip at ~100 Hz due to motor resonance. Engineers from

Superior cannot account for the differences. The torque measurements were performed by Bill delGiudice using a Prony Brake and the standard motor, translator and cables from an antenna. The different characteristics may be attributable to the long (150 feet) cable run between the translator and motor. This torque-speed data applies only to antennas 1 through 20; antennas 21 through 28 use a higher performance motor and power amplifier. The torque/speed characteristics of these components has not been measured.

In the analysis, the available motor torque was pessimistically estimated to be a constant 80% of the rated peak (1600 oz-in) value or 1280 oz-in over the 100 Hz to 400 Hz working drive rate band.

Attempts to operate the motor with loads or at speeds that exceed this torque/speed curve result in torque breakage in which the motor stops and growls. This stalled condition is tolerable for a short period and does not seem to damage the motor but can cause failure of the motor driver amplifier power transistors. The only way to recover from this stalled condition is to stop the translator switching or reduce the motor stepping rate to a level that can permit the motor to re-accelerate the drive. The new F/R Controller utilizes a ΔMotion/ΔSteps algorithm (described later) to detect the stalled condition and attempt to resume mechanism motion.

5.0 FOCUS DRIVE

The focus drive is characterized by the large translational work load imposed upon the drive motor in contrast to the relatively light inertial load.

5.1 Dead Load, vertical attitude:

Weight of Barrel and Subreflector = 540 lbs

Estimated weight of moving parts = 200 lbs

Moving assembly total weight, W_{dl} = 740 lbs

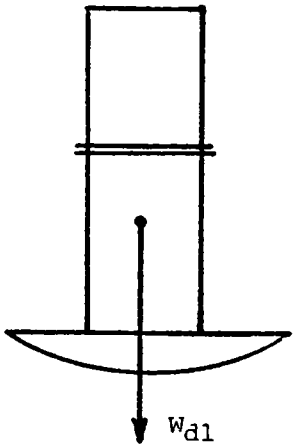

5.2 Dead Load Moment around the 4 support ball bushings, 90° tipped attitude: (counter balancing effect of counterweights is not perfect).

M_{dl} = 1375 lb-in

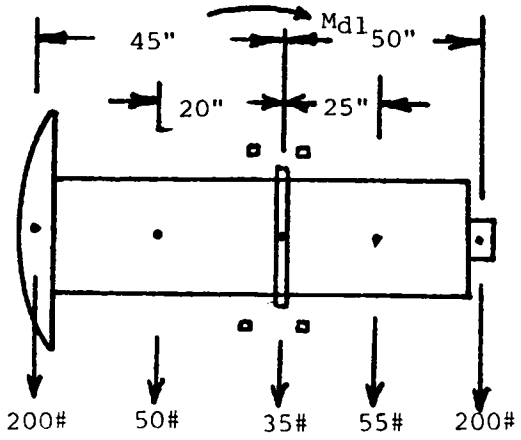

5.3 Ice load 1 cm thick (all surfaces), vertical attitude:

Surface area = 38,008 in^2

Weight of ice = 484 lbs

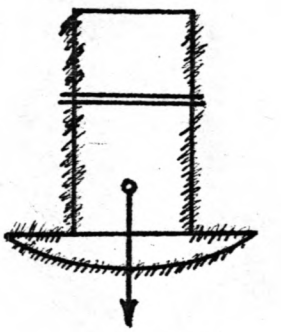

$W_{dl} + W_{ice}$

5.4 Total moment with ice load around the 4 support ball bushings, 90% tipped attitude:

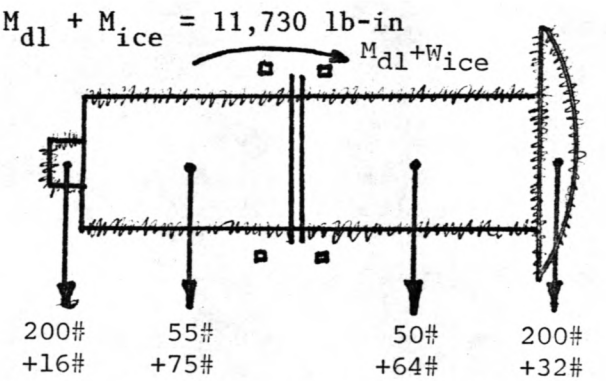

Rain and snow can accumulate in the subreflector when antennas are stowed during shutdown periods; 3 inches of water in the subreflector will create a load equal to that of 1 cm of ice. This water load has occasionally been large enough to inhibit focus drive up. Hopefully this water load will never freeze before it is dumped at observation start-up.

5.5 Wind load at 45 mph. drag coefficient of 1.5 (from Heine study), vertical attitude moment around the 4 support ball bushings at 45 mph:

M_{wind} = 3,245 lb-in

F_{wind} = 287 lb

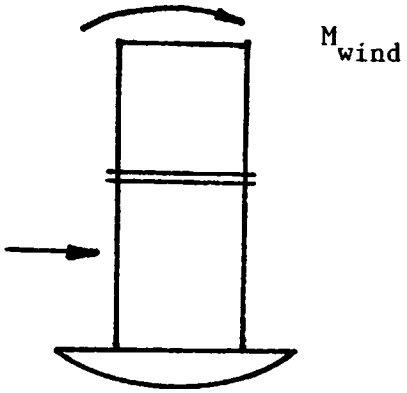

Horizontal attitude wind load:

F_{wind} = 570.3 lb, pointed into the wind.

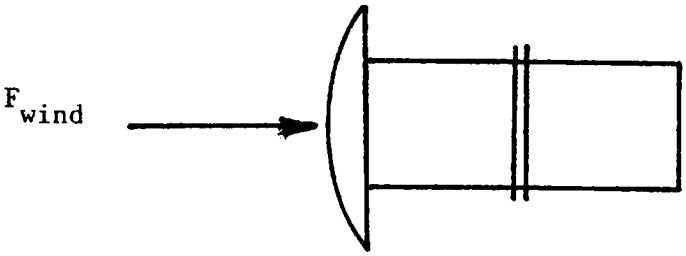

5.6 Acceleration load:

Drive Rate Profile - 100 Hz to 400 Hz in six 333 MS periods; 100 Hz, 114 Hz, 133 Hz, 160 Hz, 200 Hz, 266 Hz, and 400 Hz (new controller drive regime)

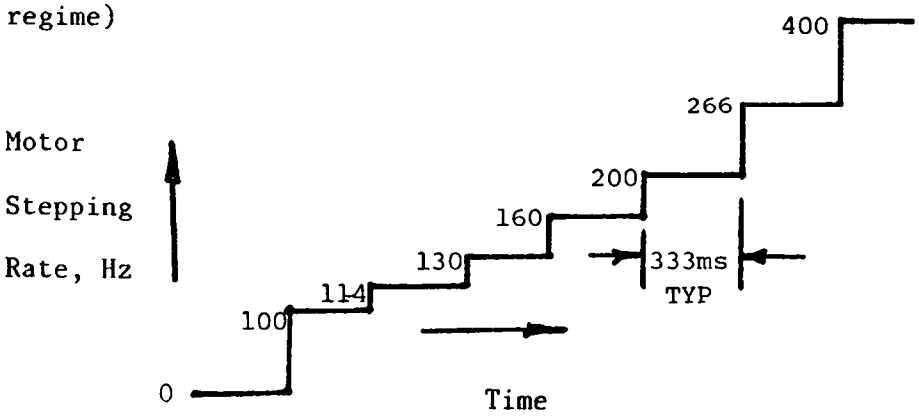

To minimize acceleration loads, the ideal stepping rate regime would be a linear smooth ramp from a few Hz to 400 Hz, but this would require that a significant fraction of the drive be done at rates under 100 Hz in the erratic drive region. The minimum desireable stepping rate is 100 Hz, (to avoid the oscillatory motion region) which necessitates a 100 Hz step at drive start that falls in the motor torque resonance dip; see Figure 3. The Model C F/R Controller drive profile depicted above features a gentle climb out of the dip and has a worst-case drive step of 134 steps/sec which occurs at the maximum of the measured torque/speed curve. The Model B F/R Controller drive profile is a 1 second smooth, linear ramp between 100 Hz and 400 Hz.

Assuming for the moment that the only inertial load imposed upon the motor is that associated with its rotor, the 1280 oz-in of torque developed by the motor can accelerate the rotor at: $T_m = I_{rot}\ \alpha_m$, = 1280/.551, = 2323 rad/sec^2, = 73949 steps/sec^2.

From the drive rate profile above, the worst-case acceleration load results from the 266 Hz to 400 Hz drive-rate step. The time required for the rotor to attain the higher velocity is: $t_o = V_m/\alpha_m$ = 1.81 Ms.

This period is less than the 266 Hz to 400 Hz step period of 2.5 Ms so the motor is capable of responding to this worst-case step speed change (not surprising). If the motor/drive coupling were rigid rather than the low spring rate elastomer coupling, the corresponding platform acceleration would be: $A_p = \alpha_m$ (.01 mm/step)(1/25.4) = 37 in/sec^2. The force which must be applied to the platform to attain this acceleration is: $F_p = (W_{dl} + W_{ice}) A_p$ = 117 lbs. The elastomer coupling will buffer this inertial force in the focus drive by "winding up" the focus coupling. Focus wind-up effects are discussed in Section i.

5.7 Maximum Motor Load

These calculations include the effects of translation, acceleration, wind, ice, and sliding friction; viscous friction is considered in the next section.

Vertical attitude, focus drive up movement.

$$L_{max} = W_{dl} + W_{ice} + F_{acc} + \mu(W_{dl} + W_{ice}) + \frac{\mu F_{wind}}{4"}$$

$$= 740 + 484 + 117 + 287 + 40$$

= 1396 lb, lifting subreflector, focus up movement. Note the dominance of the dead load and ice load.

L_{max} = 172 lb, focus down movement.

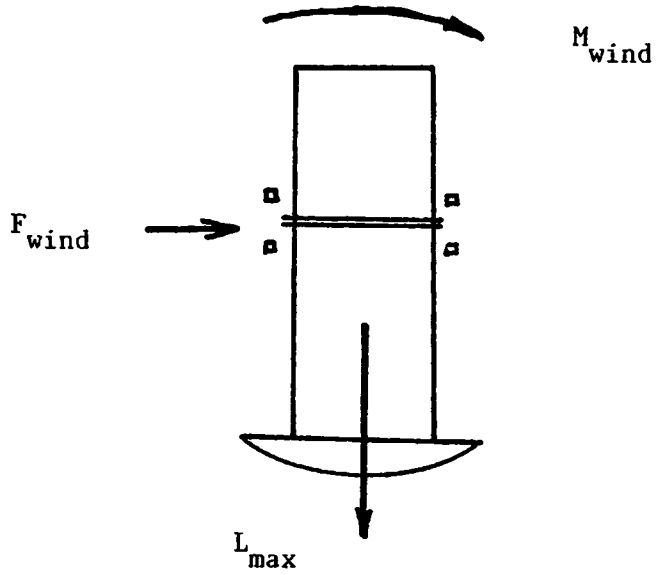

Horizontal attitude:

$$L_{max} = F_{wind} + F_{acc} + \mu(W_{dl} + W_{ice}) + \frac{\mu M_{ice}}{4"}$$

$$= 570 + 117 + 61.2 + 143.5$$

$$= 975.8 \text{ lb.}$$

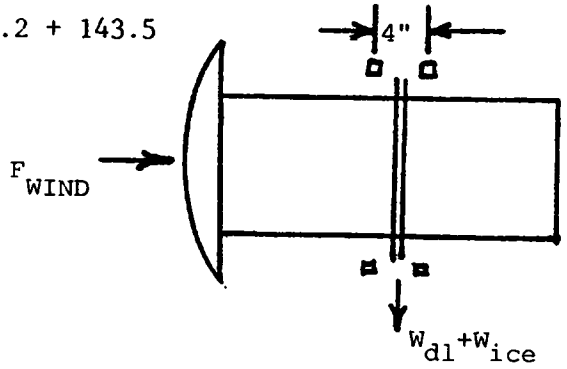

Note the dominance of the wind force.

The vertical attitude, focus drive up is the worst-case load, but there is no large difference between this and the horizontal attitude drive case. Attitudes between these two extremes will have loads which are a blend of these two cases.

The lead of the focus drive ball screw,

P_{bs} = .200 in. Torque at the ball screw (E = .9): $T_{bs} = \frac{P_{bs} L_{max}}{2\pi E}$, = 49.4 in-lb.

Estimated efficiency of ball screw drive gears: .95. Estimated efficiency of reduction gears: .975. The torque load presented to the motor, (gear ratio, i = 2.54:1) is:

$$T_{lmax} = \frac{T_{bs}}{i(.95)(.975)} = 336 \text{ oz-in.}$$

This torque load includes wind-induced and ice-induced loads. It does <u>not</u> include viscous friction loads.

5.8 Viscous Friction

Friction is a very transient quantity, always present but not constant. Antenna motion and vibration may influence drive loads in a pulsing manner, and temperature decreases will increase the viscosity of the gear lubricants. Viscous friction appears to be the dominant friction component and most intractible load in the focus drive. Many large gear surfaces are lubricated with heavy greases; a notable example is the focus drive ring gear, which has approximately 2 ft^2 of lubricated area over which viscous shear forces are developed. This gear is close to the focus drive motor and does not have a large gear ratio torque advantage in contrast to the rotation ring gear which is at the end of the gear train.

Figure 4 depicts the projected torque load imposed upon the focus drive motor as a function of temperature. The temperature-dependant dominance of viscous friction is quite evident; note the steep slope of the low-temperature region. This curve is an exponential curve fitted to the peak drag data obtained by Bill delGiudice and must be considered somewhat tentative because of the limited temperature range of the measurements and limited effort of this study. In formulating this curve, the viscous friction dependance upon velocity was ignored (drag measurements were made at a low angular drive rate); a more rigorous analysis of viscous friction would include this factor. The obvious conclusion is that this projection may be too optomistic and that the actual friction drag may be worse than pictured.

The torque margin that is available to overcome static and dynamic friction is:

$T_{marg} = T_{mot} - T_{lmax} = 1280 - 336 = 944$ oz-in.

To start mechanism motion, static and viscous friction forces must be overcome. The static friction coeffecient was estimated to be twice that of dynamic friction; therefore, if static/viscous friction loads exceed 944 oz-in, the drive will not start. Also if 472 oz-in of torque is

not available to overcome dynamic/viscous friction loads after motion has started, the mechanism will stick. Figure 4 shows that this 472 oz-in load occurs at 35° F; therefore this temperature appears to be the lower bound for successful drive under the adverse wind and ice loading environments described above. If wind and ice loading are absent, then 31° F should be the lowest operational temperature. This prediction agrees with the focus drive winter sticking experience, but unfortunately the sticking temperatures have never been recorded.

5.9 Focus Motor Coupling Torque Wind-Up

The motors are coupled to the drives by an elastomer coupling, which acts as a spring, that is deflected as a function of motor and drive load torques. The coupling is always wound up to an angle which is determined by the load torque and the coupling spring rate. Figure 5 depicts the measured torque spring characteristics of the coupling. The coupling acts as a buffer during motor acceleration in that during the first few steps of a speed change, the coupling winds (or unwinds) so that the motor is able to accelerate to a new shaft speed without having to accelerate the whole inertial load in a step-like manner.

This effect is depicted below:

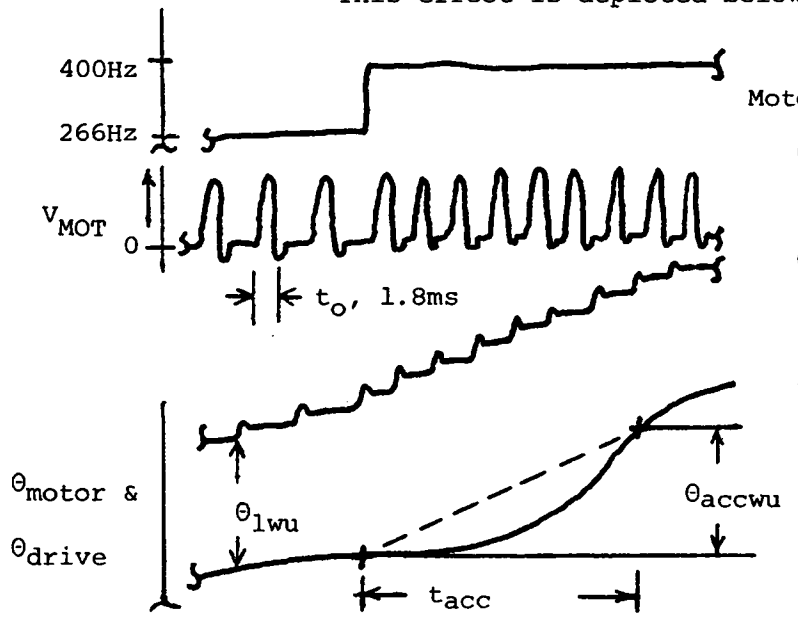

Motor Stepping Rate

Θ_{lwu} is the steady state wind-up resulting from non transient drive loads.

Θ_{accwu} is the transient wind-up resulting from changes in drive rate.

t_{acc} is the time required for the drive to accelerate to the new motor stepping rate.

The coupling wind-up phenomena also has the side effect of causing the motor to be "ahead" of the drive in terms of motor shaft motion relative to drive motion. If the drive is stopped and the brakes are engaged, the wind-up torque will be retained between the locked motor and brake. This stored torque condition currently is the case in all antennas and is the most severe in the focus drive because of the large focus-drive load. The brake may slip to relax this torque; if slipping occurs, the subreflector position will be shifted. The F/R Controller should lock the brake and relax this torque by reverse drive. This feature is not implemented in the Model B F/R Controller but is being installed in the Model C F/R Controller.

Focus wind-up calculations:

The steady state wind-up at constant speed will be determined by the frictional and translation loads. To enable acceleration of the focus drive at ~35° F, the maximum torque requirement is: $T_{max} = (L_{drive} + L_{acc}) + L_{frict}$, = 336 + 480, (from sections i and h)

= 816 oz-in

This torque load will cause a coupling wind-up of 10.90° with a K_{spr} of 268 lb-in/ rad and is a steady state value except during speed changes.

The time required to accelerate the platform during the 266 Hz to 400 Hz step is 1.81 ms. The additional motor travel during this velocity step is 134 steps/sec x 1.81 Ms = .241 steps at 1.8°/ step or .43°. Therefore the worst-case total wind-up during acceleration is 10.9° + .43° or 11.42° and is a transient condition during the step. 11.42° wind-up is equivelent to 6.3 motor steps and .85 data bits in terms of position data readout.

Coupling wind-up may be exploited as a measure of drive load and friction in that the wind-up may be dynamically calculated throughout the drive regine by counting the number of motor steps and performing a ΔMotion/ΔMotor steps

analysis. If $\Delta M/\Delta S$ is below a worst-case value during the first portion of the drive, the load is excessive and motion should be halted. A continuance of this analysis during the drive can detect excess drive friction or motor torque breakage due to excess loading. This scheme has been incorporated in the new controller drive algorithms.

Figure 6 depicts the focus coupling wind-up during acceleration and steady state drive as a function of temperature. From this curve, a maximum wind-up of 18° was chosen as an upper tolerable limit in the Model C F/R Controller; coupling wind-up values which exceed this limit are inferred to be an excessive friction or mechanism binding condition. Note that the focus steady state and transient wind-up curves are similar and close to each other; these curves and the calculations above indicate that inertial effects are not very dominant in the focus drive.

6.0 ROTATION DRIVE

The rotation drive is characterized by the large moment of inertia of the drive resulting from the use of large diameter rotating components and since it is a pure rotational system there are no translational loads. Viscous friction is less dominant in the rotation drive.

6.1 Moments of Inertia:

A) Barrel and Subreflector assembly:

I_{SR} = 871.5 lb-in-sec^2 (subreflector)

I_{CW} = 6.5 lb-in-sec^2 (counter-weight)

I_{BRL} = 118.7 lb-in-sec^2 (barrel)

I_{ASSY} = 996.7 lb-in-sec^2 (total assembly)

I_{ASSY} reflected to motor = $\frac{996 \text{ lb-in-sec}^2}{108^2}$

= .0855 lb-in-sec^2, at motor

B) Platform moveable ring: .000263 lb-in-sec^2, at motor

C) Spline Assembly: .001756 lb-in-sec^2, at motor

D) Drive Shaft, Coupling, Rotor: .03442 lb-in-sec^2, at motor

E) Total Inertial load at motor (without ice load)

$I_{TOT} = I_{BRL+SR} + I_R + I_{SPL} + I_{MOT}$

= .0855 + .000263 + .001756 + .03442

I_{tot} = .1219 lb-in-sec^2 or 1.941 oz-in-sec^2, at motor, no ice loading

Total moment of inertia with a 1 cm ice coating on all movable parts: I_{TOT} = 4.00 oz-in-sec^2.

6.2 Wind Effects

Wind effects upon the rotation drive are negligible at 45 mph.

6.3 Translation Loads

The only translation load imposed upon the rotation motor is the small off-center mass unbalance of the subreflector and very small mass non-uniformaties of the barrel/moveable ring combination; therefore the 1280 oz-in of motor torque is available for acceleration and friction loads.

6.4 Friction Loads

Using a gear efficiency of .95 for 6 meshes and the antenna friction torque measurements, an exponential curve of friction torque versus temperature was developed (again with the simplifying assumption about velocity). Figure 6 depicts this relationship. In comparing this data with the data for focus, we note that the frictional torque load imposed upon the rotation motor is much lower and is less sensitive to temperature. This prediction agrees with the much lower occurrence of cold-weather sticking in the rotation drive.

6.5 Inertial Loads and Coupling Wind-Up

In contrast to the focus drive, inertial loading is a dominant factor in the rotation drive. The buffering effect of the elastomer coupling plays a crucial role in preventing torque

breakage. From the focus inertial calculations we remember that the motor is able to accelerate the motor shaft at 73,949 steps/sec^2 with 1280 oz-in of torque. At 35° F the rotation T_{MF} is 190 oz-in (from Figure 7); thus 1280 - 190 = 1090 oz-in of torque is available for acceleration. Using α = T/I (at the load side of the coupling with an ice-loaded subreflector), α = 1090/4.0 = 272.5 rad/sec and is the maximum possible drive acceleration at this temperature. With this torque the time required to accelerate the subreflector during the worst-case 266 Hz to 400 Hz drive rate step is: $t_o = \dot{\theta}/\alpha$ = (134)(1.8)/(272.5)(57.3), = 15.5 Ms or the period of six motor steps. If the motor drive coupling were rigid, the motor would problably break torque and stall, but with the elastomer coupling the motor is able to continue stepping by winding up the coupling while the drive accelerates to the new drive rate. For this case the motor must rotate ahead (wind-up) of the coupling by: θ_{cwu} = (1090)/(286)(16), = .254 radians to develop enough torque to accelerate the drive. This wind-up will require (.254)(57.3)/(1.8) = 8.09 motor steps. During these steps the drive will be accelerating but we will assume for simplicity of analysis that the drive will only "see" the acceleration torque of 1090 oz-in at the

8th motor step at which time the drive will begin acceleration to the 400 Hz rate which requires 15.5 Ms or 6 motor steps. The total wind-up (acceleration) time is then t_{acctot} = 35.5 Ms or 14 motor steps at 400 Hz. The worst case difference between Θ_{motor} and Θ_{drive}, Θ_{accwu} is 8 motor steps or 14.4°. The drive load-associated wind-up, Θ_{dl} is: Θ_{dl} = (190)/(268)(16), = .0443 radians. The total wind-up $\Theta_{totwu} = \Theta_{accwu} + \Theta_{dl}$, = .251 + .0443, = .295 radians, (16.9°) or 9.4 motor steps. This is equivelent to 9.4 minutes of subreflector position, and 1.5 data bits in terms of position readout. Wind-up values (differences between the translator switching and realized drive motion) which exceed 11 motor steps are inferred to indicate an excess friction condition by the ΔM/ΔS algorithm in the Model C F/R Controller. This wind-up analysis is depicted below: (not drawn to scale)

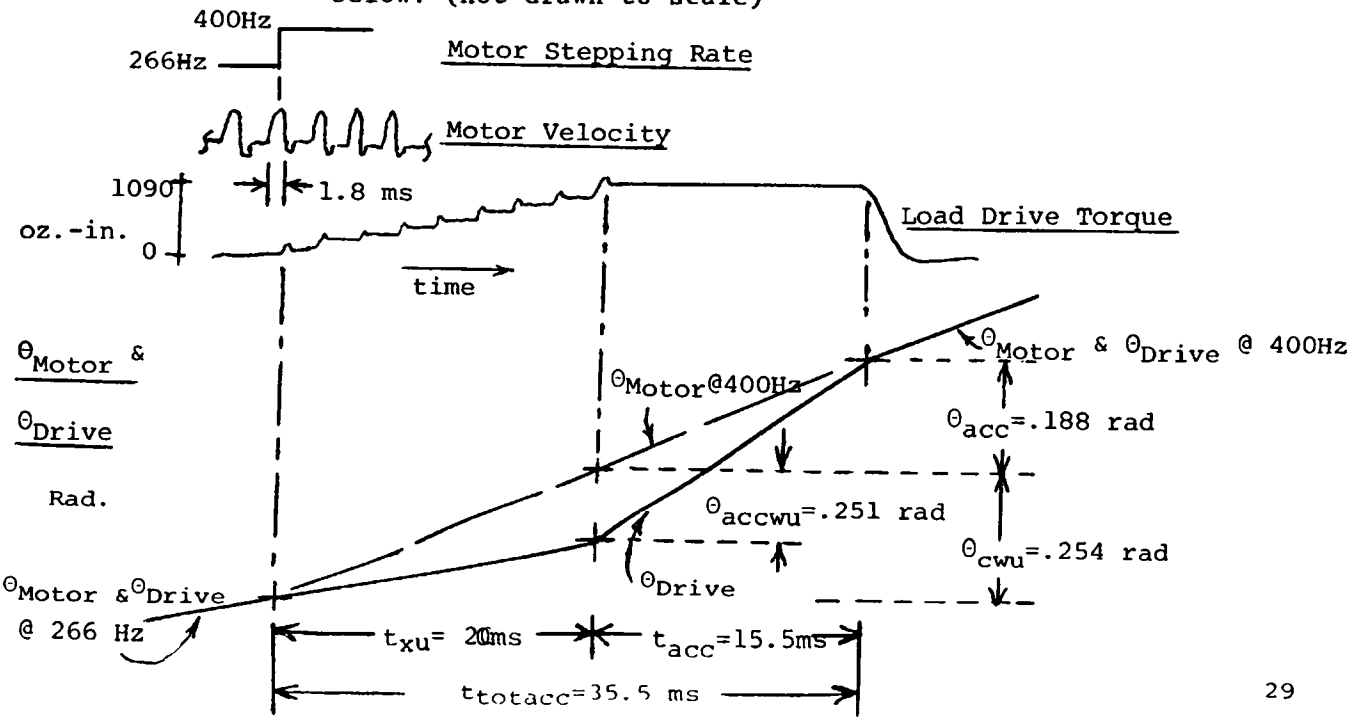

If the motor were to be rigidly coupled to the drive, the acceleration associated with the 266 Hz to 400 Hz step would be: $\alpha = 2\theta/t_o^2 = (2)(1.8)(57.3)/(2.5 \times 10^6)^2$, $= 33 \times 10^6$ rad/sec, at the motor. The motor torque required to accelerate the load would be: $T = I\alpha$, $= (4.0$ oz-in $sec^2)(33 \times 10^6$ rad/$sec^2)$, $= 132 \times 10^6$ oz-in which exceeds the available torque. These values indicate the sensitivity of the rotation drive to acceleration effects.

7.0 CONCLUSIONS

Based upon the analysis, measurements and operational experience, the suggested bounds and environmental constriants of the F/R Drive are as follows.

7.1 Temperature - 30° F is suggested as a low bound if sleet or freezing rain is not present and 35° F when it is present. No practical high temperature limiting conditions are known.

7.2 Drive Speed - Motor drive speed should be restricted to the 100 to 400 Hz region because of the erratic drive motion and 550 Hz torque fall-off described above.

7.3 Motor Torque Load - No load should exceed the 80% of rated torque value of 1280 oz-in.

7.4 Attitude - Although no measurements of friction drag at any attitude other than vertical are known by the writers, the analysis indicates that under the conditions described and with the assumed friction coefficients, the motors develop adequate torque to properly operate the drives at any attitude between 0° and 90° tipping above the 30° or 35° temperature bounds.

7.5 Time Since Major Overhaul - This parameter was not analyzed but one of the writers has noted considerable rust and dirt deterioration of the drive bearings in the F/R Mounts which have been disassembled for repair and renovation. These and other components degradation must add a significant but unknown load to the motor drive burden.

7.6 Antenna Drive Motion and Vibration - This parameter was not analyzed but can affect static and dynamic friction coefficients and induce larger than normal force loads upon mechanism components.

7.7 Wind - Wind load effects up to 45 Mph are tolerable. Wind effects above 45 Mph were not calculated.

7.8 Accuracy - This analysis did not address this topic, but it appears that the worse-case interpretation of the specifications cited in VLA Technical Report No. 42, F/R System should apply. Gear and mechanism wear will degrade the positional and readout accuracy of the mechanism.

7.9 Rain - Normal rainfall should not affect the drive when the antenna is active during observations, but rain can accumulate if the antenna is stowed during shut-downs. A small amount of rainwater (3") in a stowed antenna subreflector can inhibit focus drive in the up direction. The subreflector has drain holes to prevent this accumulation, but they can become plugged by bird dung; perhaps a bird dung purge function should be added to the F/R Mount.

8.0 RECOMMENDATIONS

8.1 The temperature dependance of friction drag should be evaluated at temperatures down to -10° F.

8.2 Friction drag should be measured in both drives for several tipping attitudes down to horizontal.

8.3 The drag or sticking effects of an ice-loaded brake should be evaluated.

8.4 The torque/speed characteristics of the new (Antennas 21-28) drive motors should be measured.

8.5 Friction drag of the drives should be measured before disassembly when the F/R Mounts are removed from the antennas for renovation.

8.6 This memorandum and the analysis should be reviewed by those who have an interest in the F/R Drive dynamics.

8.7 If cold weather sticking occurs again this winter, the telescope operators should note the time, temperature, and weather conditions under which it occurred.

8.8 The effect of mechanism wear and lost motion (slop) upon readout accuracy should be analyzed.

8.9 The mechanical design should be reviewed to attempt to devise means by which the torque margins can be improved. Two suggestions are: use lower viscosity lubricants and decrease the pitch of the focus drive ball screws.

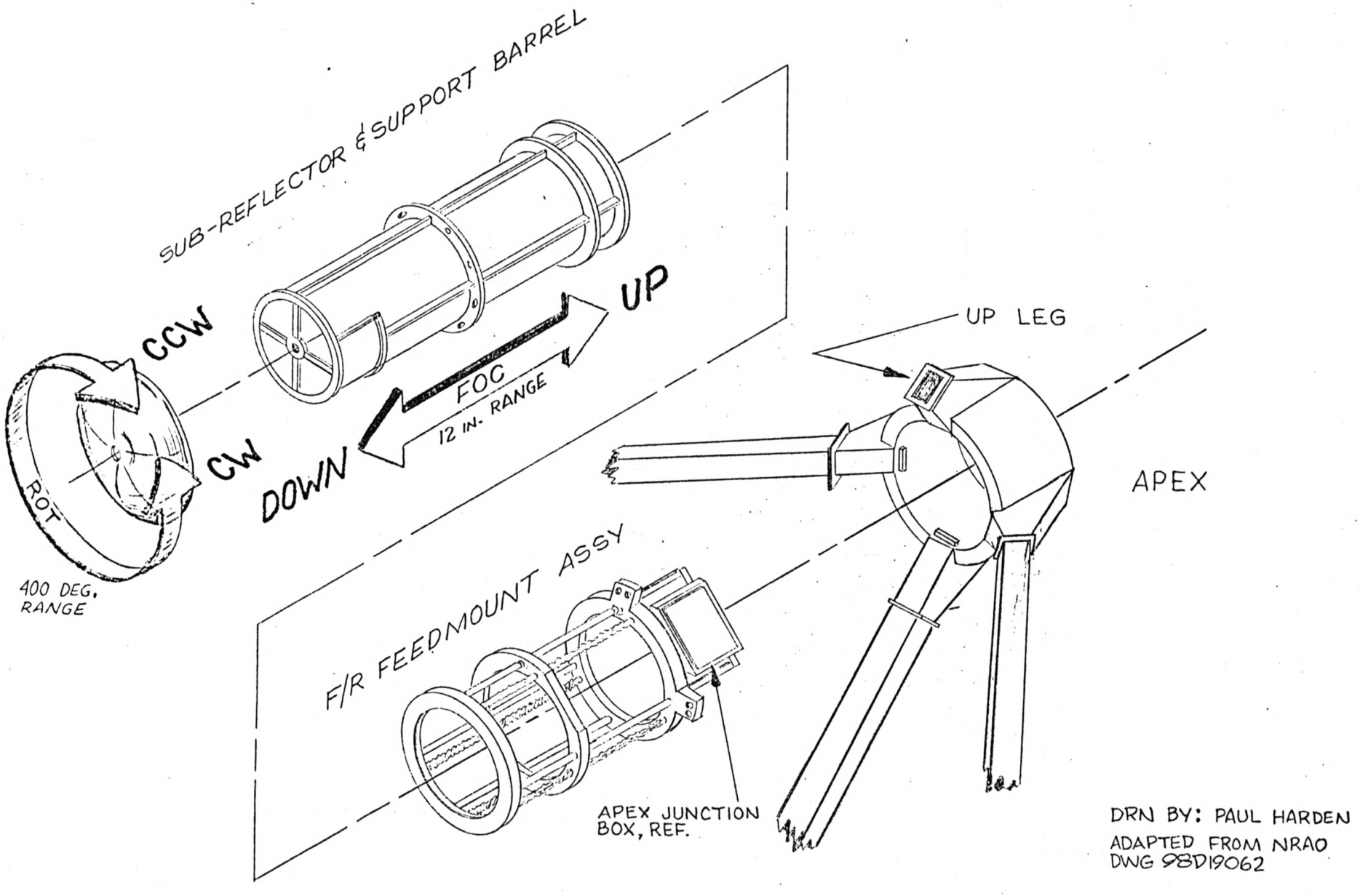

FIG. 1 - SUBREFLECTOR MOUNT & DRIVE, ISOMETRIC ASSEMBLY

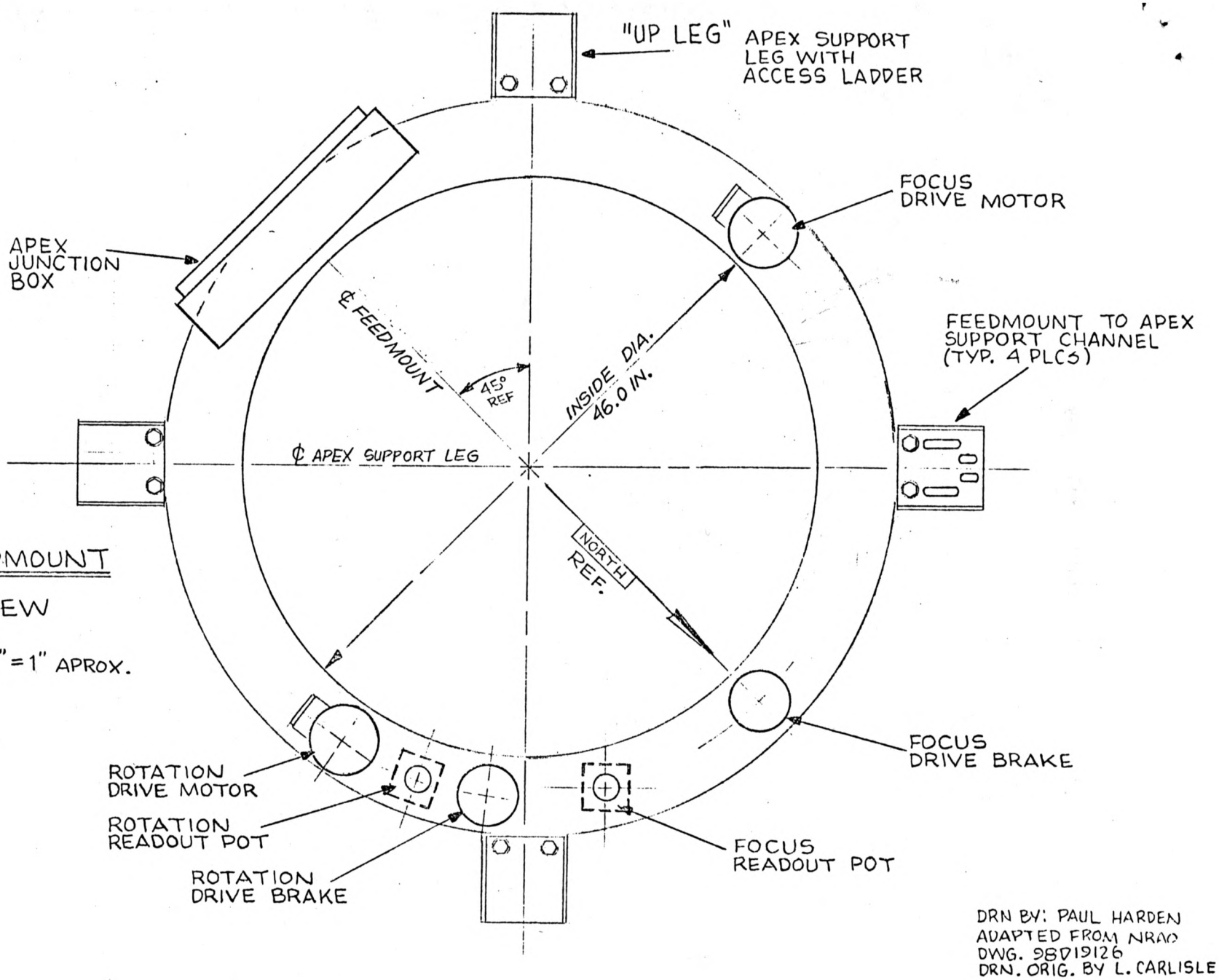

FIG. 2 - F/R MOUNT, DRIVE AND CONTROL COMPONENTS

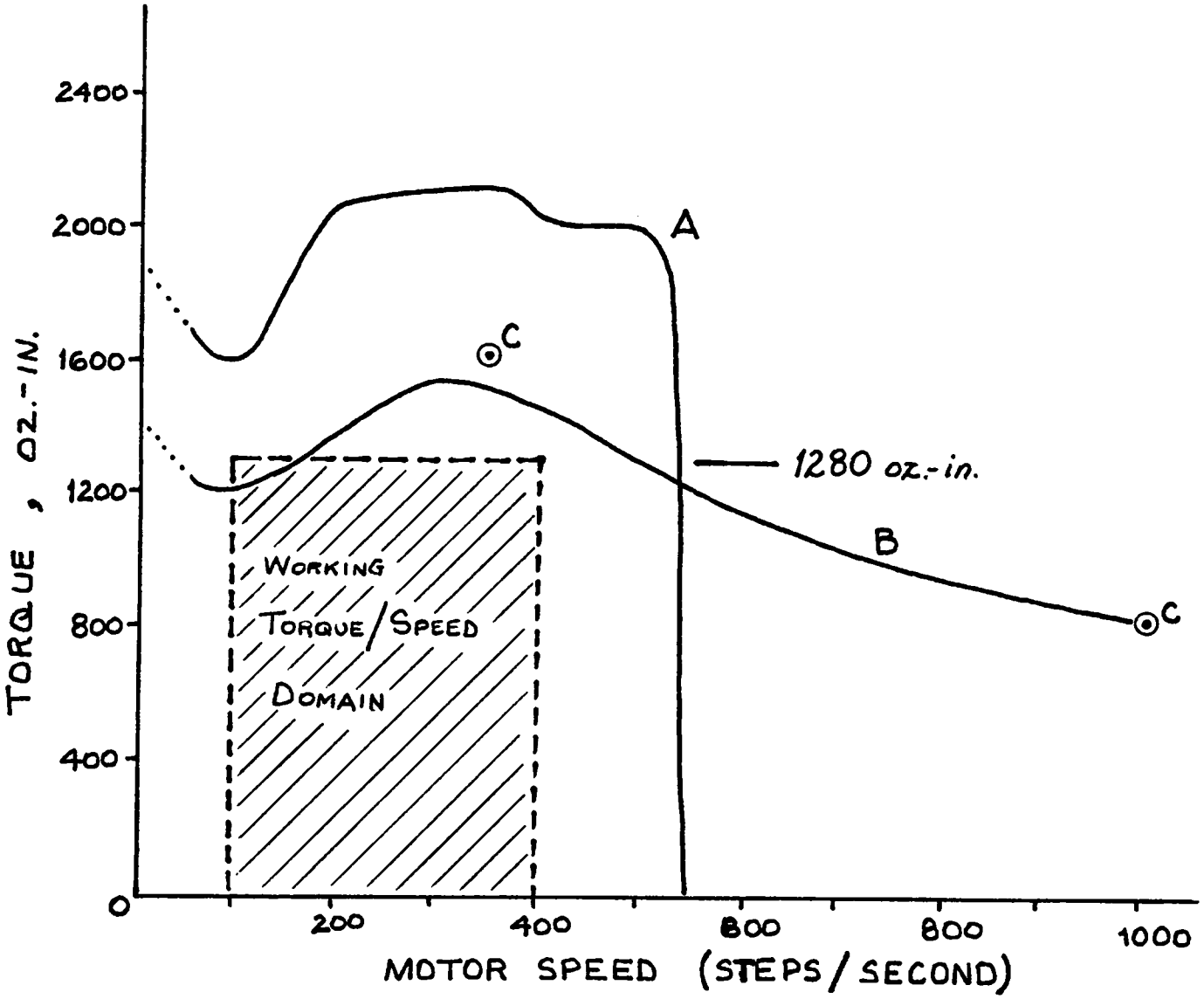

FIGURE 3.

A = Measured Speed/Torque Characteristics, 3/31/80-BDG

B = NTR 1500-NS 1500 Speed/Torque Characteristics, Superior Electric Data

C = Torque Points for HTR1008 Translator/NS1500 Motor, NRAO Purchase Order Specification Points.

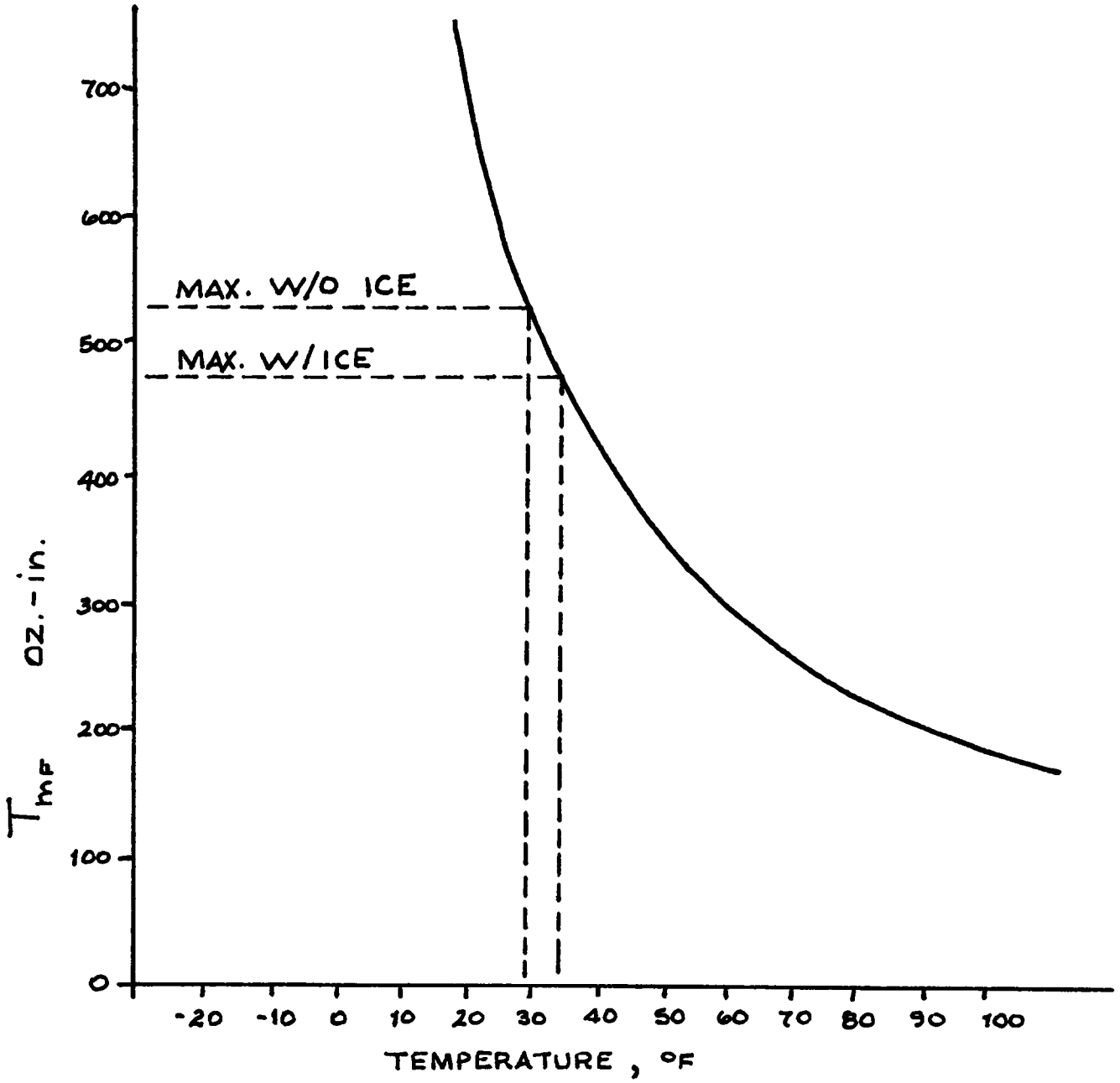

FIGURE 4. FOCUS FRICTION TORQUE AS A FUNCTION OF TEMPERATURE

(Data taken from memo (L. Temple to D. Weber 4-11-80.) Measurements were made with antenna stowed, little wind, and no ice. Peak torque readings were used for this plot.)

DATA VALUES

TORQUE, OZ-IN	DEFLECTION, DEG.
480	8
960	17
1440	25
1920	38
2880	64

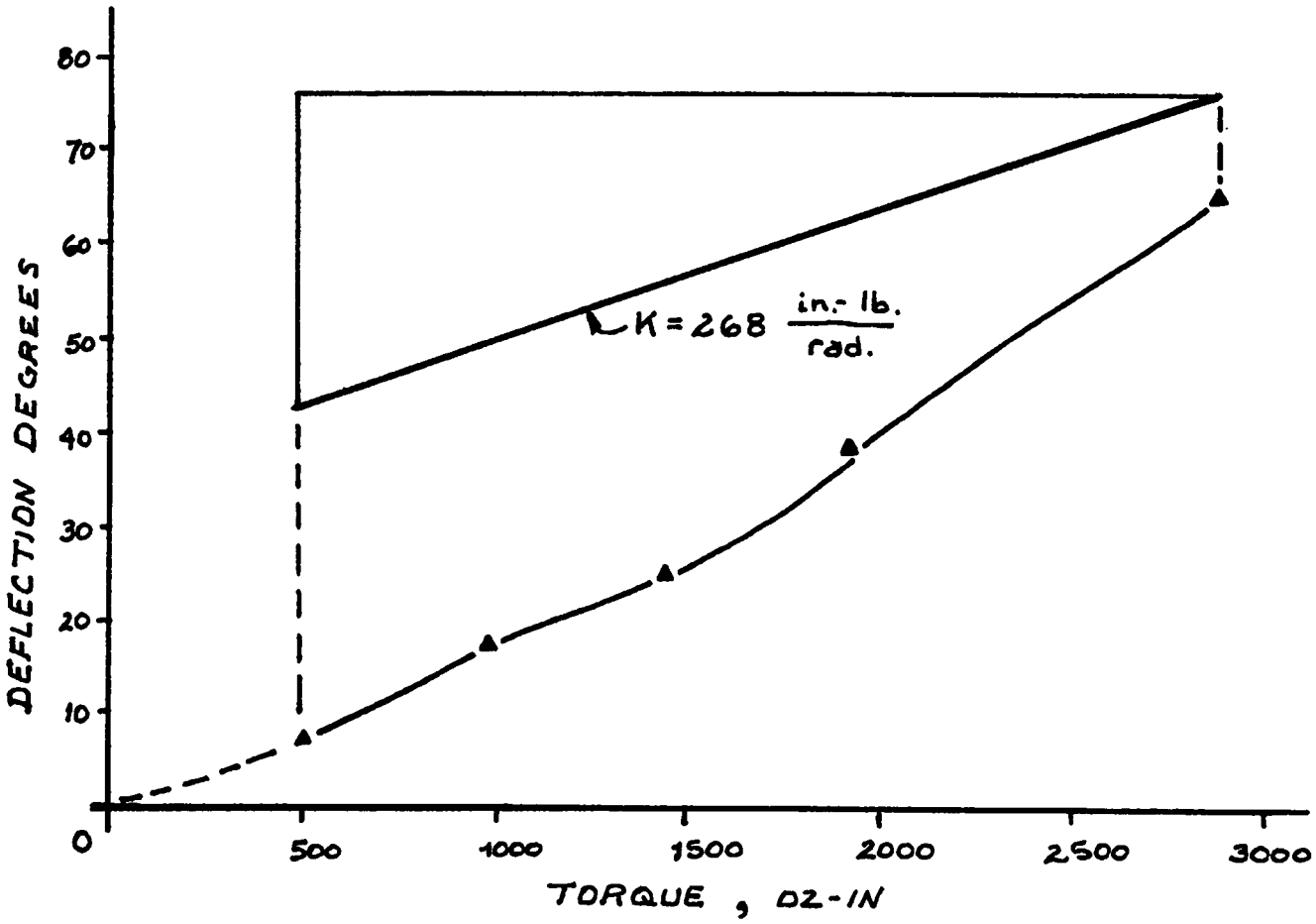

FIGURE 5. MOTOR COUPLING WIND-UP AS A FUNCTION OF TORQUE

Coupling: LORD # J-1211-7-9

(Data taken from memo, (L. Temple to D. Weber 4-11-80.) Measurements were made with antenna stowed, little wind, and no ice. Peak Torque readings were used for this plot.)

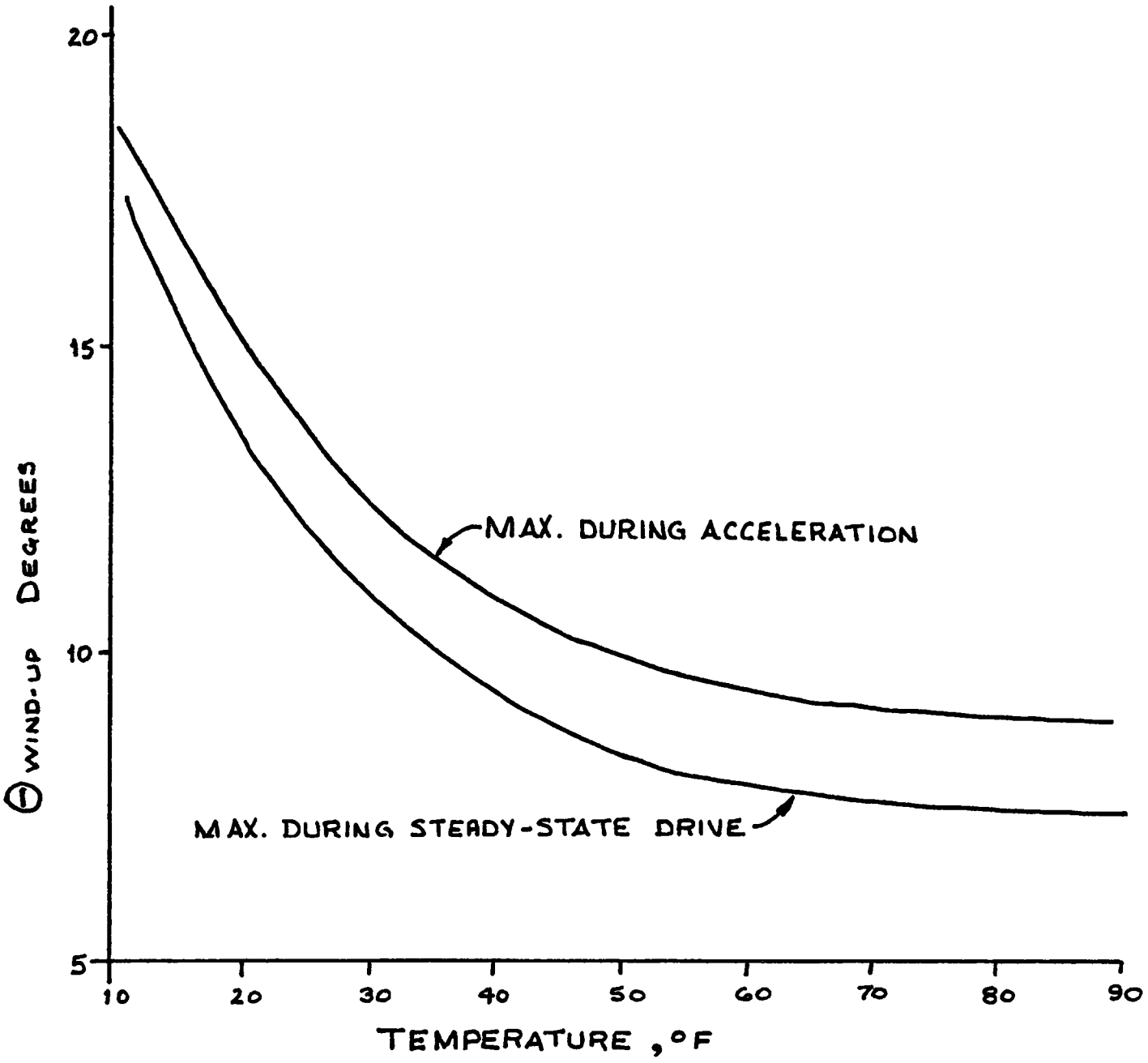

FIGURE 6. FOCUS COUPLING WIND-UP, Θ, AS A FUNCTION OF TEMPERATURE.

(Focus Drive Up, Vertical Attitude. Worst Case, Wind and Ice Loads.)

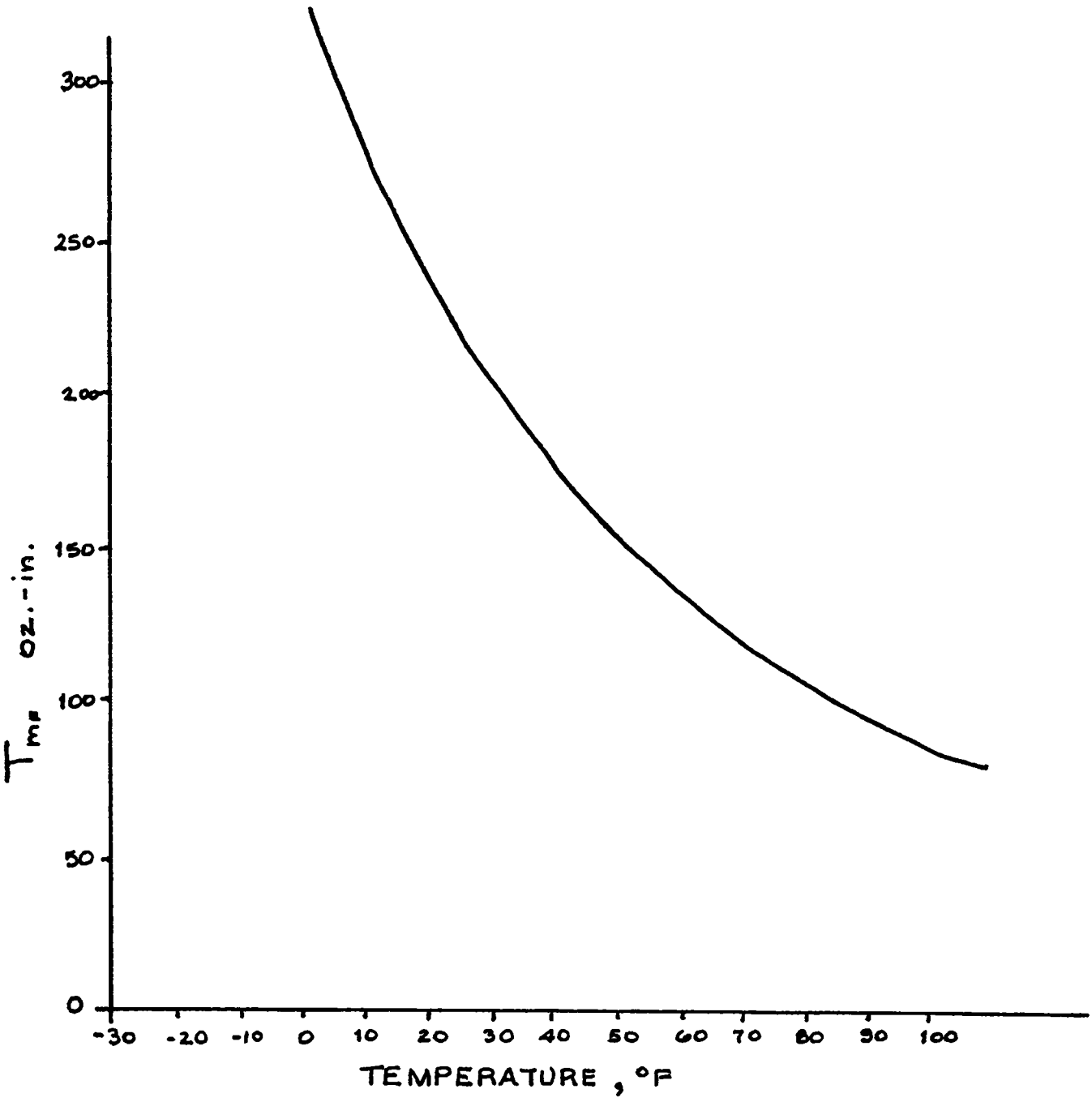

FIGURE 7. ROTATION FRICTION TORQUE AS A FUNCTION OF TEMPERATURE

(Data taken from memo, (L. Temple to D. Weber 4-11-80.) Measurements were made with antenna stowed, little wind, and no ice. Peak torque readings were used for this plot.)

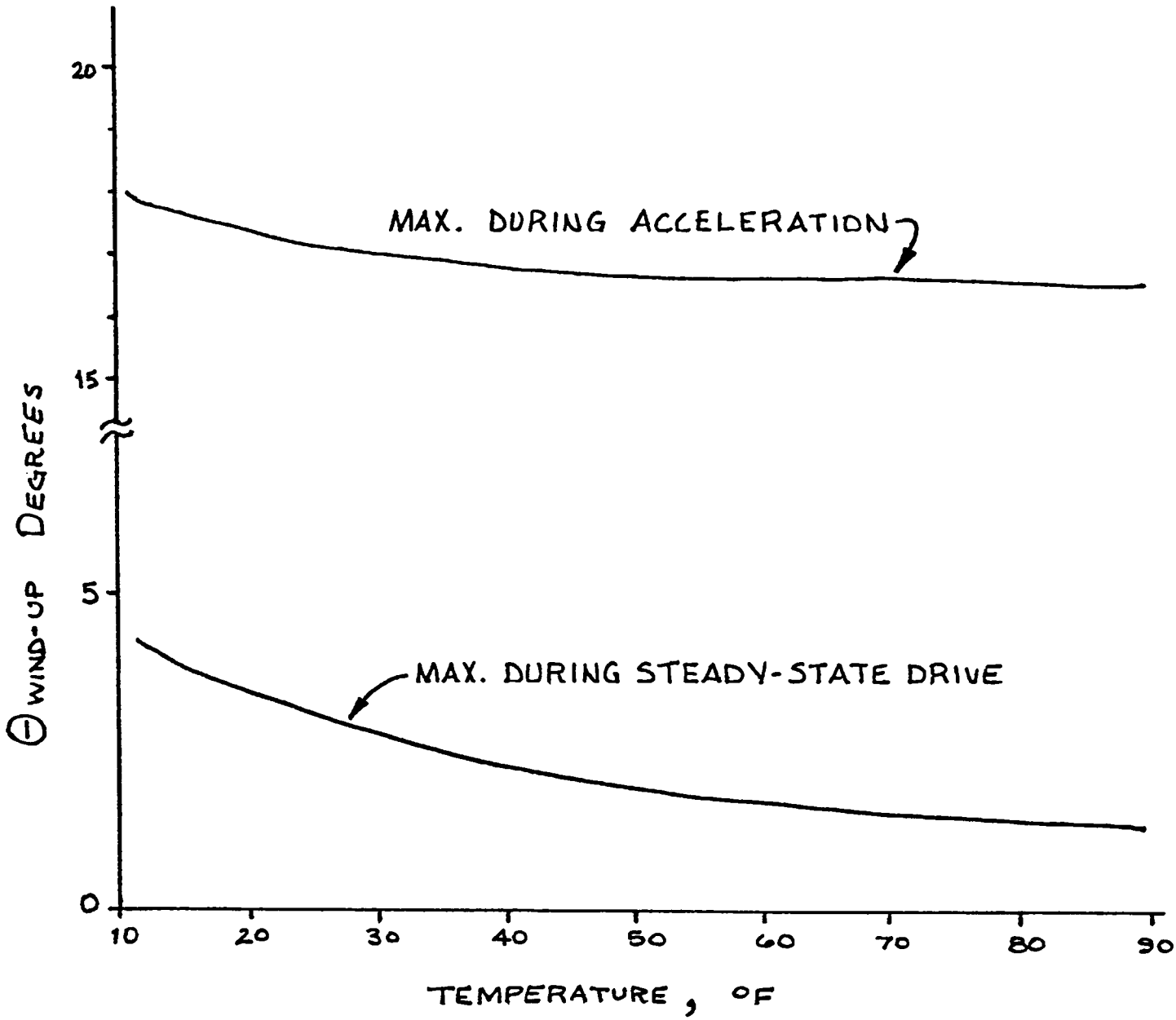

FIGURE 8. ROTATION COUPLING WIND-UP, Θ, AS A FUNCTION OF TEMPERATURE

(Worst Case, Wind and Ice Loads)